# MICROEXPLOSION OF EMULSIFIED FUEL DROPS

A. Elgowainy and N. Ashgriz

## ABSTRACT

The explosion dynamics of a liquid drop driven by a high-pressure bubble is simulated numerically by solving the full two-dimensional Navier-Stokes equations and exact boundary equations. It is shown that bubble surface roughness generated by Landau instability during the rapid evaporation stage of the internal phase significantly affects the hydrodynamics instability of the subsequent stage. This study suggests that Rayleigh-Taylor instability controls the hydrodynamics of the subsequent stage and affects the microexplosion disruptive phenomenon and the drop breakup time. The numerical investigation demonstrates the effects of surface tension, viscosity, pressure and size of the internal phase, and characteristics of interfacial disturbance on the internal phase growth, the bubble surface phenomena and the drop breakup time.

## INTRODUCTION

The phenomenon of microexplosion is often observed during the combustion of fuel emulsions and multi-component fuel droplets, which are made up of two or more liquids with relatively large differences between their boiling temperatures. The microexplosion may occur when the superheat limit of the interior phase (which is far above the boiling point and is about 10% below the critical temperature for many substances) is lower than the saturation temperature of the surrounding phase. Intense disruption occurs due to the rapid evaporation of the droplet interior phase by spontantaneous homogeneous nucleation which results in a high pressure bubble inside the liquid phase (Shepherd and Sturtevant 1982). The bubble grows violently causing the disruption of the liquid drop into small secondary drops in a process known as secondary atomization or microexplosion. The concentration and physical properties of the droplet components as well as the size of the internal drops and their interior locations determine the severity of the liquid disruption (Lasheras *et al*. 1981, Marrone *et al.* 1983). The microexplosion of fuel droplets is very effective in reducing the unburned soot particles, which are formed when burning heavy fuel oils, by producing smaller fuel droplets and better spray dispersion. Shepherd and Sturtevant (1982) observed that the bubbles generated by homogeneous nucleation have large amplitude small-scale rough surface during most of the evaporative stage which is in contrast of the smooth bubbles observed in conventional boiling and is attributed to the Landau instability accompanying the rapid evaporation process. After the rapid evaporation of the internal phase, a liquid droplet entrapping a high-pressure bubble with small-scale perturbation at their interface is expected, Fig. 1.

In this paper, an accurate numerical model is employed to simulate the hydrodynamics of microexplosion following the evaporation stage and its effect on the breakup time of an emulsified liquid droplet. The surface perturbation produced by the rapid evaporation process stimulates the development of Rayleigh-Taylor instability in the subsequent stage. The Rayleigh-Taylor instability dominates the hydrodynamics of this stage and affects the disruptive phenomena and the drop breakup time.

Rayleigh-Taylor instability is a fingering instability of an accelerated interface between two fluids of different densities. An extensive review of the Rayleigh-Taylor instability phenomenon and its applications is given by Sharp (1984). Elgowainy and Ashgriz (1997) studied in details the stages of instability development in viscous fluid layers by solving the full nonlinear Navier-Stokes equations and using an accurate model (FLAIR) for interface reconstruction.

In this paper we consider a simple model of an emulsified fuel drop composed of a fuel drop entrapping a more volatile droplet as shown in Fig. 1. The perturbation at the interface represents the instability generated by the rapid evaporation process of the internal phase. The parameters of interest to this study are, the bubble size, the thickness of the liquid layer entrapping the bubble, the interfacial surface tension, the viscosity of the fuel drop, and the perturbation characteristics at the interface. The liquid layer thickness is inversely proportional to the number density of the dispersed phase in an emulsified fuel drop. Initially, the size of the internal phase is small with high radius of curvature. This results in a small inertia to surface tension ratio, i.e., low Weber number. As the bubble expands, the inertia forces develop rapidly with a consequent increase in Reynolds number and Weber number, thus resulting in a rapid development of the interfacial instability. This paper investigates the effects of the interfacial perturbation, the initial bubble size and the fluid properties on the breakup time of the liquid drop.

## PROBLEM FORMULATION

Figure 1 shows a schematic of a liquid drop with a bubble at its center. A single mode perturbation is imposed initially at the interface according to the equation, $r = A\cos(4fs/r_m)$, where $A$ is the initial amplitude of perturbation, $s$ is the axis of perturbation along the interface, $4f$ is the number of interfacial perturbation cycles, and $r_m$ is the initial mean radius of the bubble. The initial radius of the drop, $R$, is the natural length scale for this problem. The fluid layer is initially at rest and is accelerated by the internal pressure, $P_i$. The outer surface of the drop is exposed to zero pressure; thus $P_i$ represents the pressure difference across the liquid layer. After proper scaling of the variables, the governing equations of the problem can be written as follows,

$$\frac{\partial u_i}{\partial x_i} = 0$$

$$\frac{Du_i}{Dx_i} = X_i - \frac{\partial p}{\partial x_i} + \frac{\partial \tau_{ij}}{\partial x_j}, \text{ where, } \tau_{ij} = \frac{1}{Re}\left(\frac{\partial u_i}{\partial x_j} + \frac{\partial u_j}{\partial x_j}\right)$$

The boundary conditions can be written as follows:

$$1 + (\tau_{ij})_{surface}\, n_i n_j = \frac{1}{We\, R_c}$$

$$(\tau_{ij})_{surface}\, n_j s_i = 0$$

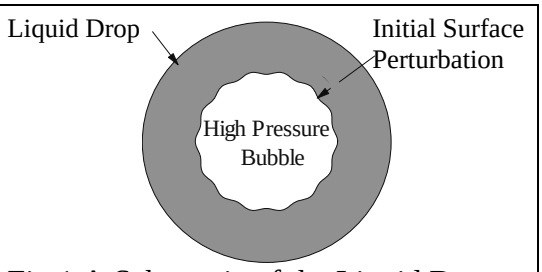

Fig.1 A Schematic of the Liquid Drop

In these equations the dimensionless variables are defined as,

$$x = \frac{x'}{R},\ y = \frac{y'}{R},\ u_i = \frac{u_i'}{\sqrt{P_e/\rho}},\ t = \frac{t'\sqrt{p_i/\rho}}{R},\ Re = \frac{R\sqrt{\rho P_i}}{\mu},\ We = \frac{RP_i}{\sigma},\ X_i = \frac{RX_i'}{P_i/\rho},\ R_c = \frac{y_{xx}}{(1+y_x^2)^{\frac{3}{2}}},\ A = \frac{\varepsilon}{R}$$

In the above equations, $u_i$ is the local velocity vector, $Re$ is the Reynolds number, $We$ is the Weber number, $P_i$ is the internal pressure, $n_i$ is the unit vector normal to the interface with

horizontal component $n_x = -y_x/(1+y_x^2)^{1/2}$ and vertical component $n_y = 1/(1+y_x^2)^{1/2}$, $s_i$ is the unit vector tangent to the interface with horizontal component $s_x=n_y$ and vertical component $s_y=-n_x$, $R_c$ is the local radius of interface curvature, $A$ is the dimensionless amplitude of the initial perturbation, $R$ is the initial drop radius, $\rho$ and $\mu$ are the density and viscosity of the liquid layer, respectively, $\sigma$ is the interfacial surface tension, $X_i$ is the gravitational body force, $y_x$ *and* $y_{xx}$ are the local first and second derivatives at the interface, respectively. The Weber number measures the relative competition between the internal pressure force and the capillary force. The capillary force is determined by the size of the internal phase, which depends on the emulsion structure, and by the interfacial surface tension. The initial bubble radius represents the concentration of the internal phase as a volume percentage of the total drop size.

## RESULTS

Validation of the adapted numerical scheme requires quantitative agreement with independent experiments or analytical solutions. Our results are validated against the analytical solution of the perturbation equations in the linear regime. The accuracy of our calculations is also verified by the symmetric evolution of the growing instability as well as the conservation of the total mass in the liquid layer. A symmetric evolution of the growing perturbation proves the numerical results to be independent of the grid orientation. The results have also been verified to be independent of grid sizes smaller than the size necessary for resolving the largest interfacial deformation. The mass is conserved to accuracy within $10^{-3}$ to$10^{-4}$ for all our numerical calculations. Several restrictions are placed on the time step and the grid size to ensure the stability of the results. Our calculations show no evidence of numerical instability.

Figure 2 shows the growing interfacial instability at high Weber number (*We*=1000) and Reynolds number (*Re*=200). The internal phase undergoes rapid expansion due to the internal pressure forces and is accompanied by growing surface perturbation in the form of Rayleigh-Taylor instability. The internal phase expansion and the growing interfacial instability contribute to the thinning of the liquid layer, leading to the breakup of the liquid drop. The drop breakup time is calculated as a function of Weber number as shown in Fig. 3. The plot shows a lower limit of Weber number below which the breakup time does not significantly increase since the liquid layer breaks solely due to stretching in the absence of interfacial instability. The plot also shows a higher limit of Weber number above which the breakup time does not significantly decrease due to the negligible effect of surface tension on the instability growth.

The spike amplitude of the growing perturbation (measured from the mean radius of the internal bubble) is plotted at different Weber numbers in Fig. 4. The figure indicates that the instability growth rate is reduced when the Weber number is decreased due to the effect of surface tension in hindering the internal phase growth and impeding the instability development. At low Weber number, the surface tension forces become large enough to regress the initial amplitude from positive to negative as in the case of *We*=30, Fig. 4. As the Weber number is further reduced, the perturbation amplitude oscillates in time between positive and negative as in the case of *We*=20. The interface oscillates due to the competition of surface tension and inertia forces. This is demonstrated in Fig. 5 by the interchanging position of the perturbation's heads and tails with time. The bubble keeps growing until the liquid layer is thin enough to break, mainly due to stretching. At low Weber numbers, the drop breaks due to the internal phase growth. At high

Weber numbers, there is an added contribution from the instability development to the layer thinning process. The contribution from the instability growth results in a smaller size of the internal phase at the breakup time of the drop.

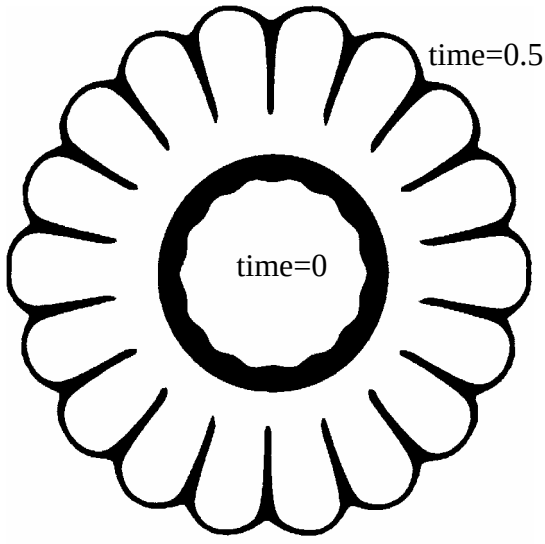

Fig. 2 Instability development at We=1000

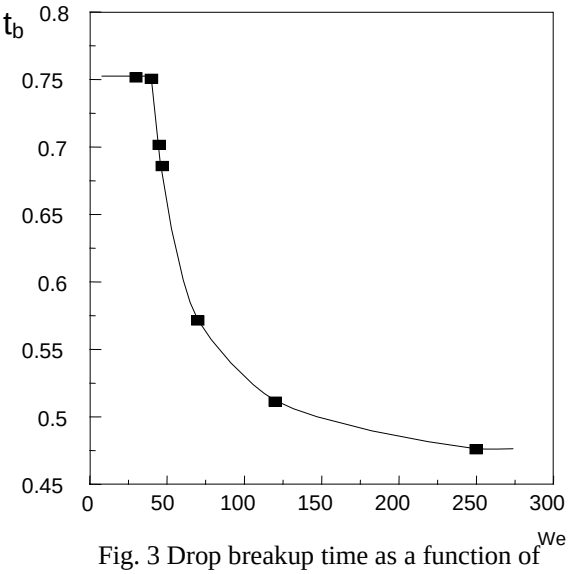

Fig. 3 Drop breakup time as a function of Weber number

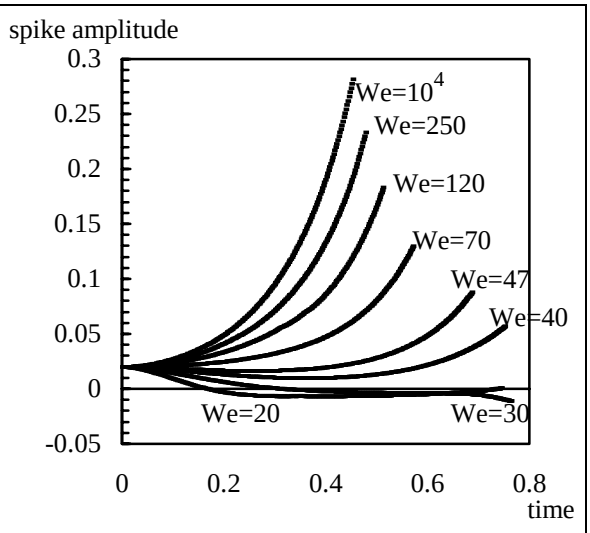

Fig. 4 Spike growth rate at different Weber number

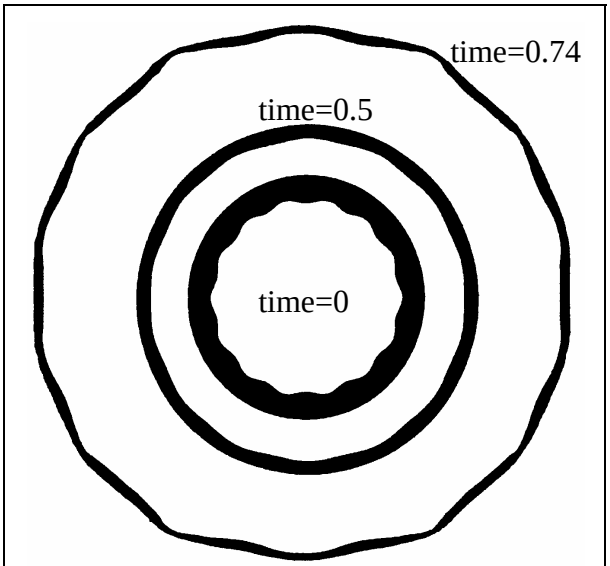

Fig. 5 Instability development at We=25

Figure 6 shows the growth rate of the mean radius of the internal phase at initial bubble radii of 0.5, 0.7 and 0.8. The drop breakup time increases as the bubble radius decreases, Fig. 7. This is due to the increase in the inertia resistance of the surrounding drop to the instability development, the increase in the time required to stretch a more massive drop, and the increase in surface tension forces due to the increase in the local curvature of the interface. Figure 7 shows that, for the selected range of bubble radii at $We=10^4$, the breakup time changes linearly with the bubble radius. This leads to a zero breakup time when the bubble radius is extrapolated to its upper limit of 1.

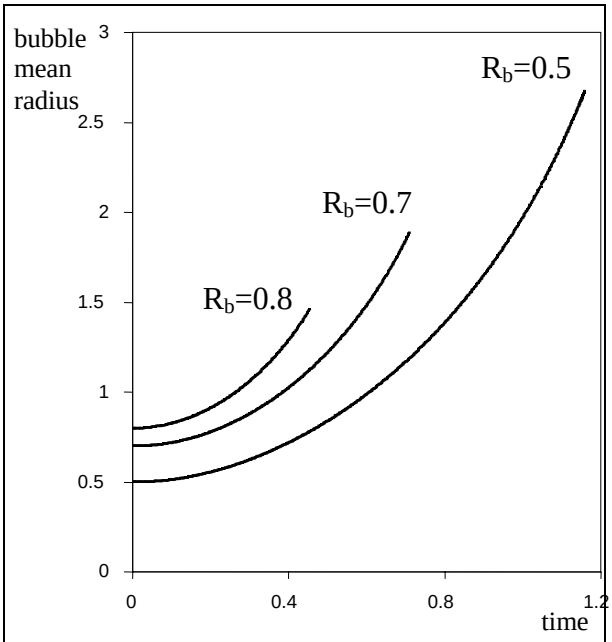


Fig. 6 Bubble growth rate at different initial bubble radii

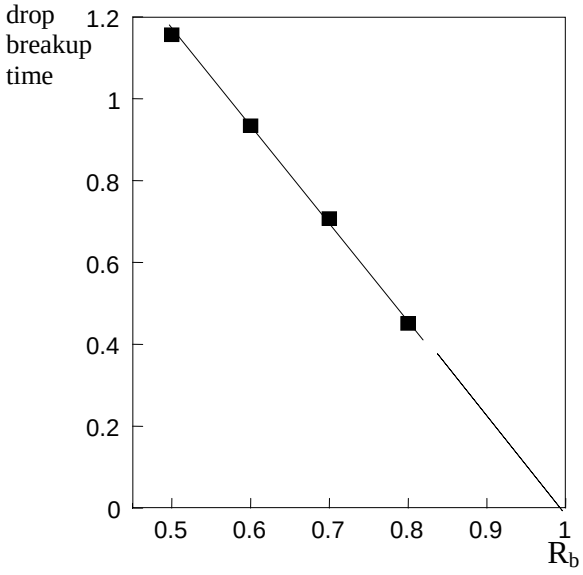


Fig. 7 Drop breakup time as a function of initial bubble radius

Surface perturbations with higher frequency modes are shown to reduce the drop breakup time significantly, Fig. 8. This is attributed to the existence of more sites for growing spikes, which enhance the contribution of the instability growth to the layer thinning rate and the drop breakup time. The thinning of the liquid layer and its progressive effect on the instability growth are the primary reasons for the early disruption of the liquid drop. It should be noted that at low Weber number, the surface tension forces play important role in stabilizing higher frequency modes. Consequently, higher frequency modes may or may not be favorable for the microexplosion process depending on the value of Weber number.

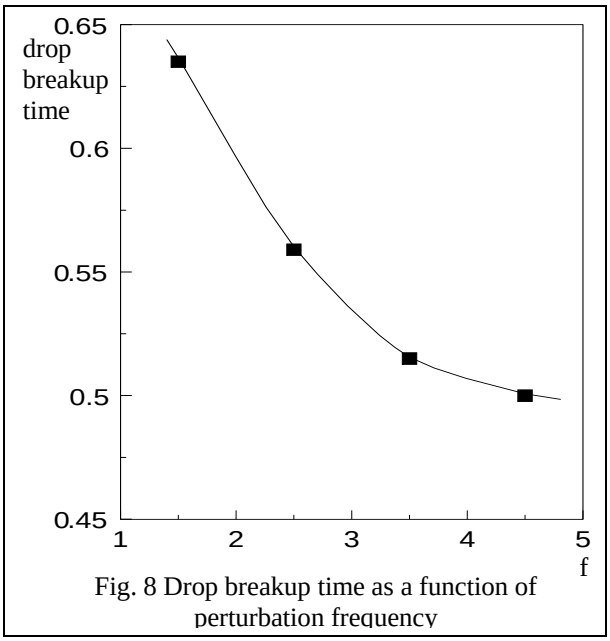


Fig. 8 Drop breakup time as a function of perturbation frequency

## CONCLUSIONS

The explosion dynamics of a liquid drop driven by a high-pressure bubble is demonstrated through a numerical simulation. The drop breakup time is evaluated as a function of Weber number, perturbation frequency and initial bubble size. Both the bubble expansion and the instability growth contribute to the thinning rate of the liquid layer and the drop breakup time. At high Weber and Reynolds numbers, the surface instability grows rapidly and reduces the drop

breakup time significantly. Higher frequency modes enhance the layer's thinning rate and drop breakup is shortly observed. The breakup time is found to increase linearly with the initial size of the internal phase.

## REFERENCES


[1] J. E. Shepherd and B. Sturtevant, Rapid Evaporation at the Superheat Limit, *J. Fluid Mech.* **121**, (1982) 379-402.

[2] J. C. Lasheras, A. C. Fernandez-Pello and F. L. Dryer, On The Disruptive Burning of Free Droplets of Alchol /n-Paraffin Solutions and Emulsions, *Eighteenth Symposium (International) on Combustion,* The Combustion Institute, (1981) 293-305.

[3] N. J. Marrone, I. M. Kennedy and F. L. Dryer, Short Communication: Internal Phase Size Effects on Combustion of Emulsions, *Combustion Science & Technology* **33**, (1983) 299-307.

[4] D. H. Sharp, An overview of Rayleigh-Taylor instability, *Physica* **12D**, (1984) 3-18.

[5] A. Elgowainy and N. Ashgriz, The Rayleigh-Taylor Instability of Viscous Fluid Layers, *Phys. Fluids* **9**, (1997) 1635-1649.